*Zuerst ersch. in : APL Materials ; 1 (2013), 4. - 042109*
*http://dx.doi.org/10.1063/1.4824040*

# Synergistic effects of interfacial modifiers enhance current and voltage in hybrid solar cells

Jonas Weickert,[1] Eugen Zimmermann,[1] Julian B. Reindl,[1] Thomas Pfadler,[1] James A. Dorman,[1] Annamaria Petrozza,[2] and Lukas Schmidt-Mende[1,a]
[1]*Department of Physics, University of Konstanz, POB 680, 78467 Constance, Germany*
[2]*Center for Nano Science and Technology @Polimi, Istituto Italiano di Tecnologia, Via Pascoli 70/3, 20133 Milano, Italy*

To unleash the full potential of hybrid solar cells, it is imperative to get significant photocurrent contribution from both the sensitizing dye and the polymeric hole transporter. Here we report on the interfacial modifier 4-mercaptopyridine (4-MP), which induces controlled orientation of poly(3-hexylthiophene) (P3HT), the most widely used hole transporting polymer for hybrid solar cells, at the interface. 4-MP optimizes the charge separating interface between P3HT and a squaraine dye-decorated $TiO_2$, inducing enhanced contribution to photocurrent generation by the polymer. In combination with 4-*tert*-butylpyridine, which enhances the open circuit potential in dye-sensitized and hybrid solar cells but reduces the photocurrent, a synergistic effect is observed and it is possible to enhance both open circuit voltage and photocurrent simultaneously. Similar effects on device performance are also found for two other commonly used dye molecules, a fullerene derivative and a common indoline dye. 

Hybrid metal oxide-polymer solar cells represent an emerging technology that holds the advantage of pronounced difference in dielectric constants of electron donor and acceptor compounds, controllable phase separation, and chemical stability compared to conventional organic photovoltaic.[1] A widely used geometry for hybrid solar cells consists of a dye-sensitized nanostructured $TiO_2$ electrode processed from a nanoparticle paste, which is infiltrated with a strongly absorbing hole transporting polymer.[2–4] Typically, this polymer is a polyphenylene vinylene[5] or poly(3-hexylthiophene) (P3HT),[6] which is the current baseline donor polymer in organic solar cell research.[7,8] P3HT forms highly ordered crystallites when in its regio-regular configuration.[9] Crystalline P3HT exhibits additional absorption features due to $\pi$-$\pi$ stacking between polymer chains, extending the absorption spectrum up to 650 nm.[10] Furthermore, the hole mobility of P3HT is increased significantly during crystallization, especially in $\pi$-$\pi$ stacking direction and along the polymer backbone.[11] In order to maximize the efficiency of P3HT-based photovoltaics, it is imperative to control the orientation of the P3HT crystallites. Recently, Canesi *et al.* reported on a massive efficiency improvement of hybrid solar cells based on bare $TiO_2$ and P3HT using the modifier 4-mercaptopyridine (4-MP).[12] This pyridine self-assembles into a monolayer on the $TiO_2$ surface and induces a face-on alignment of P3HT, giving rise to significantly improved charge separation efficiencies and resulting in improved short circuit current density ($J_{SC}$). Thus, they were able to boost the efficiency from 0.37% to 0.95% and even further to 1.13% after thermal annealing of the polymer.

Here we report on the application of 4-MP in hybrid solar cells based on dye-sensitized $TiO_2$ electrodes with P3HT as hole transporter. A monolayer of 4-MP is deposited via a simple spincoating and subsequent washing after dye-sensitization of the $TiO_2$ nanoparticle electrode and before deposition of the hole transporting polymer. In our devices, incorporation of 4-MP enhances photocurrent

[a]Author to whom correspondence should be addressed. Electronic mail: lukas.schmidt-mende@uni-konstanz.de

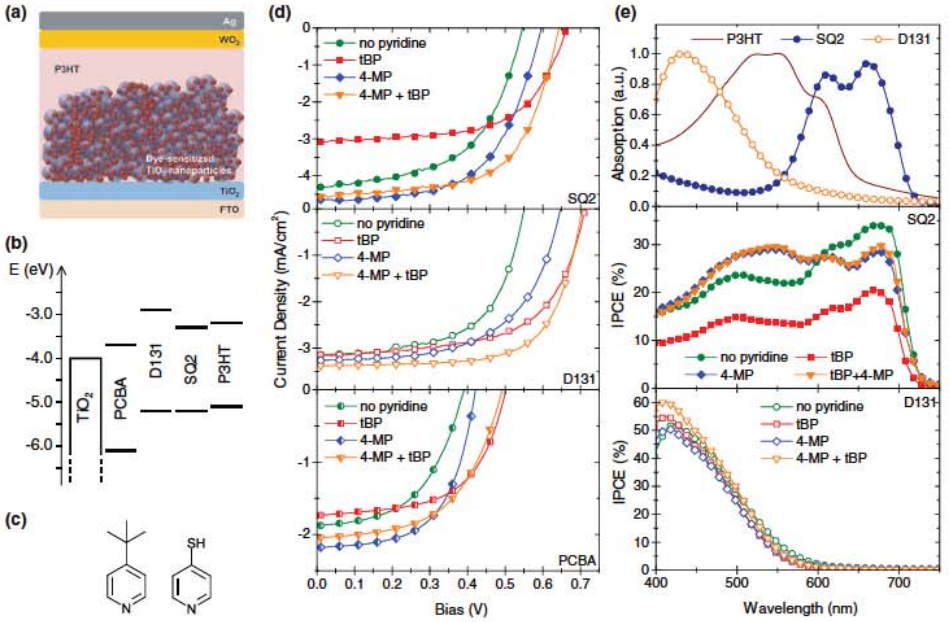


FIG. 1. (a) Schematic of the solar cell geometry used in this study. (b) Energy diagram of $TiO_2$, PCBA, D131, SQ2, and P3HT. Energy levels from Refs. 2, 3, 8, and 16. (c) Chemical structures of the two pyridines tBP (left) and 4-MP (right) used as interfacial modifiers. (d) Current density-voltage curves for solar cells with different pyridine configurations and the dyes SQ2, D131, and PCBA (from top to bottom). (e) Typical absorption spectra of P3HT on glass and $TiO_2$ nanoparticle films sensitized with SQ2 and D131 (top), and IPCE spectra of solar cells with different pyridine configuration with SQ2 and D131 as sensitizer.

generation and reduces charge carrier recombination, which we attribute to favorable orientation of P3HT at the interface. Our results show that 4-MP can be employed as an interfacial modifier in addition to other widely used interfacial modifiers, specifically 4-*tert*-butylpyridine (*t*BP), to enhance the open circuit voltage ($V_{OC}$) by inducing a shift of the $TiO_2$ conduction band edge.[13,14] While this enhanced $V_{OC}$ usually comes at the price of a reduced photocurrent, we find that *t*BP and 4-MP show a synergistic effect that simultaneously improves $J_{SC}$ and $V_{OC}$, especially for dyes which allow photocurrent contribution of the polymer. Enhancing the current contribution of the polymer is an important step towards increased efficiency of hybrid solar cells, which to date rely mainly on the contribution of the dye.[15]

A schematic of the geometry of fabricated solar cells is shown in Figure 1(a). A dye-sensitized $TiO_2$ nanoparticle film (approximately 500 nm film thickness) is deposited over a $TiO_2$ compact layer on a fluorine-doped tin oxide substrate. The $TiO_2$ electrode is infiltrated with P3HT, processed from an *ortho*-dichlorobenzene solution and used without any annealing steps. A hole selective 8 nm thick $WO_3$ interlayer is thermally evaporated[17] and the solar cell is finalized with an evaporated 150 nm thick Ag electrode. A detailed description of the solar cell fabrication procedure and the measurement techniques can be found in the supplementary material.[18]

In this study we show the positive effect of 4-MP on the device performance for three different dye molecules, a squaraine dye (SQ2), a yellow dye (D131), and a fullerene derivative (PCBA).[18] SQ2 is chosen since it is a close relative of SQ1, which has shown remarkable efficiencies in combination with P3HT on $TiO_2$ nanotubes as reported by Mor *et al.*[16] Additionally, D131 has been reported by Zhang and co-workers to allow efficiencies approaching 4%, the highest value to date for a $TiO_2$-dye-P3HT hybrid device.[2] Finally, PCBA, introduced by Vaynzof *et al.*, is a modified [6,6]-phenyl-$C_{61}$-butyric acid methyl ester (PCBM) buckminsterfullerene with a carboxyl linker group. It has shown more than 100% enhanced charge injection from P3HT into ZnO.[19] Using PCBA, significantly increased photocurrent has also been shown for P3HT on $TiO_2$.[20] In 2012, Grancini and co-workers showed efficient hybrid solar cells using a carboxylated fullerene as sensitizer on $TiO_2$ using PCPDTBT[21] as hole transporter.[22] Energy levels of the materials are shown in Figure 1(b).

Four different configurations were tested for each dye molecule to evaluate the impact of 4-MP on the device performance. Specifically, the four configurations are: no interfacial modifier as a reference, modification with *t*BP, modification with 4-MP, and finally a co-modification with both *t*BP and 4-MP. The 4-MP layer is applied after dye-sensitization via spincoating and subsequent washing in order to form a self-assembled monolayer. For the co-modified configuration, *t*BP is deposited first and 4-MP is applied on top. The actual mixing ratio is therefore unknown, but we assume that our processing results in a mixture of 4-MP and tBP on the surface since both molecules attach with the pyridine moiety to the $TiO_2$ and we expect similar binding energies for the two molecules. We also find similar results when spincoating a 1:1 mixture of *t*BP and 4-MP but choose a step-wise processing, which we find to give more reproducible solar cell devices. Chemical structures of *t*BP and 4-MP are shown in Figure 1(c). Atomistic simulations performed by Canesi *et al.* showed that 4-MP forms a highly ordered monolayer with the sulfhydryl groups pointing away from the $TiO_2$, enabling the alignment of the P3HT alkyl side chains along the thiol rows with the polymer backbone lying planar on the $TiO_2$ surface.[12] Therefore, the P3HT assembles in a face-on configuration, implying intimate contact between the polymer chromophores and the charge separating interface, as well as high hole mobility through the P3HT crystal perpendicular to the interface.

Current density-voltage curves under illumination with a 100 mW $cm^{-2}$ Air Mass (AM) 1.5G solar simulator are shown in Figure 1(d) for the different configurations. Solar cells are kept in a light-tight metal holder covering the side and backsides of the devices to ensure that light is coupled in only through a shadow mask defining the active area of the device. Thus, overestimation of the $J_{SC}$ is avoided as described by Snaith.[23] Power conversion efficiency (PCE), $V_{OC}$, $J_{SC}$, and fill factor (FF) for typical devices are summarized in Table ST1 in the supplementary material.[18] The measurements show enhanced $V_{OC}$ after a *t*BP post-treatment of the $TiO_2$ for all dyes ($V_{OC}$ increases by 21%, 29%, and 28% for SQ2, D131, and PCBA, respectively), which is consistent with literature. A significant reduction of the $J_{SC}$ by 28% and 7% is measured for SQ2 and PCBA, respectively, whereas the $J_{SC}$ is not affected in case of D131. We attribute these differences to the position of the different lowest unoccupied molecular orbital (LUMO) levels of the dyes with respect to the P3HT. For D131, charge injection from the P3HT is impossible due to the lower LUMO of P3HT, which has already been discussed by Zhang *et al.*[2] However, for SQ2 and PCBA, the polymer can contribute to the photocurrent generation, as apparent from incident photon to current conversion efficiency (IPCE) plots shown by Mor *et al.* and Vaynzof *et al.*, respectively.[16,19] For the fullerene, the polymer comes into play via charge injection into the PCBA, whereas a Förster resonance energy transfer is supposedly occurring between the SQ2 and P3HT. Application of *t*BP induces a dipole moment at the interface, which reduces the driving force for electron injection and supposedly for charge separation between P3HT and PCBA. Furthermore, *t*BP might physically space the polymer away from the dye molecule. This could explain the relatively strong effect in case of SQ2, since the efficiency of an energy transfer depends strongly on the distance between donor and acceptor.

When using 4-MP as interfacial modifier, we find a systematic increase in both $V_{OC}$ and $J_{SC}$, consistent with the results for bare $TiO_2$.[12] The slight change in $V_{OC}$ is attributed to a shift in $TiO_2$ conduction band edge similar to the case of *t*BP, since 4-MP has a dipole moment, which points in the same direction but is smaller than that of *t*BP.[24] For SQ2 and PCBA, which allow contribution from the polymer, the $J_{SC}$ is enhanced by 10% and 9%, respectively, whereas for D131 the increase is only 4%. Additionally, a significantly improvement in FF was measured for PCBA with 4-MP modification.

The striking result of this study is that the best solar cells are obtained for a combination of *t*BP and 4-MP. Using a 1:1 mixture of the two pyridines, the $V_{OC}$ can be increased by 18%, 28%, and 26% for SQ2, D131, and PCBA, respectively. Furthermore, when co-modifying with the two pyridines the $J_{SC}$ simultaneously increases, in contrast to modification only with *t*BP. Thus PCE enhancements of at least 40% were measured for the *t*BP and 4-MP combination, compared to solar cells without pyridine modifiers. We attribute this to a synergistic effect of the two pyridines, where *t*BP induces an increased $V_{OC}$ while 4-MP maintains a high $J_{SC}$ due to favorable alignment of the P3HT at the interface.

The impact of 4-MP on the photocurrent generation is also apparent from IPCE spectra, as shown in Figure 1(e). SQ2 and D131 both absorb complementary to P3HT, D131 in the blue and

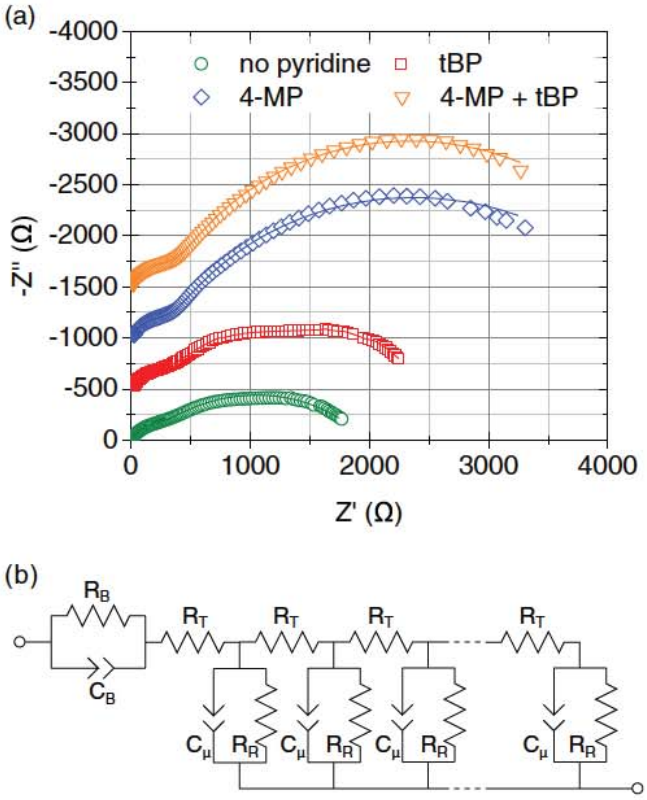


FIG. 2. (a) Nyquist plot of impedance spectra recorded for SQ2 solar cells with different pyridine configurations. Data are acquired at 0 V bias and under white light illumination with approximately 100 mW $cm^{-2}$. Curves are offset in 500 Ω steps in Z″ direction. Lines represent fit results using the (b) equivalent circuit model for a mesoporous hybrid solar cell (fits are performed with ZView).

SQ2 in the red. Therefore, the contribution of dye and polymer can be easily distinguished in the IPCE. For SQ2, there is a clear P3HT feature in the IPCE next to the SQ2 peak. Interestingly, for solar cells with 4-MP, the relative contribution of P3HT is enhanced, whereas the dye contributes relatively more than the polymer in devices without 4-MP. We attribute this to 4-MP induced polymer orientation at the interface, which enables more efficient charge separation upon P3HT excitation. In contrast, the shape of the IPCE is not affected by the choice of pyridines for D131. The total absence of a P3HT feature suggests that charge injection from the P3HT into the dye is still energetically forbidden even if the polymer is nicely oriented.

We also performed photoluminescence (PL) spectroscopy measurements on samples with SQ2 and different pyridine configurations. PL quenching can give a hint on how efficiently charge separates at interfaces.[25] For our samples we find the lowest PL emission without pyridine and similar, slightly higher PL intensity with pyridines.[18] We attribute this to reduced direct contact between P3HT and $TiO_2$ due to the presence of additional pyridine covering the $TiO_2$ between the dye molecules. Direct contact between $TiO_2$ and P3HT quenches the polymer's emission, although a $TiO_2$-P3HT interface does not separate charges very efficiently without additional interfacial modifiers.[14,20] Further investigation with time resolved spectroscopy is necessary in order to identify mechanisms involved in charge separation at 4-MP modified dye-polymer interfaces. This, however, is not within the scope of this communication.

In order to characterize the electronic properties of the pyridine modified interfaces, impedance spectroscopy measurements were performed for the SQ2 sensitized devices.[18] Spectra were recorded at 0 V bias and under illumination with a white light diode at approximately 100 mW $cm^{-2}$. A Nyquist plot of the recorded spectra is shown in Figure 2(a). Data were fitted using an equivalent circuit

TABLE I. Impedance spectroscopy fit results (fits with ZView) for recombination resistance and constant phase element parameters (capacitance $Q_n$ and capacitor ideality factor n) representing the $TiO_2$-P3HT interface for different pyridines.

| | No pyridine | tBP | 4-MP | 4-MP + tBP |
|---|---|---|---|---|
| $R_R$ (kΩ) | 181 ± 3 | 244 ± 3 | 418 ± 6 | 401 ± 5 |
| $Q_n$ (nC) | 55.1 ± 3.2 | 46.6 ± 2.3 | 9.9 ± 0.4 | 5.5 ± 0.3 |
| n | 0.57 ± 0.01 | 0.57 ± 0.01 | 0.74 ± 0.01 | 0.79 ± 0.01 |

model similar to the one used by Zhang *et al.* for $TiO_2$-D131-P3HT hybrid solar cells.[2] In order to get good fitting results the model was extended by one additional R-constant phase element (CPE) component, which is associated with the polymer capping layer and the interface between polymer and top contact, in accordance with literature.[26] The resulting equivalent circuit is shown in Figure 2(b). The $TiO_2$-organic interface is described by the parallel R-CPE units in the transmission line part of the equivalent circuit, where $C_\mu$ describes the chemical capacitance of the interface and $R_R$ is associated with a recombination resistance.[27] Fit results for these elements are summarized in Table I. Our results show that modification of the interface with 4-MP leads to significantly increased recombination resistances as compared to bare $TiO_2$ and *t*BP. High $R_R$ is also maintained when 4-MP is combined with *t*BP. Furthermore, the chemical capacitance is significantly reduced and higher values of n are found in presence of 4-MP. Although further research including a detailed impedance spectroscopy study at different illumination intensities and bias voltages is necessary to clarify the origin of this behavior, we believe that the 4-MP-induced P3HT alignment can lead to a lower number of interface trap states and the crystallinity of the polymer at the interface is supposed to improve the local charge mobility, which reduces charge carrier recombination.[28]

The reduced interfacial recombination suggested by impedance measurements is also supported by slightly improved charge carrier collection efficiencies $\eta_{coll}$.[29] Transient photocurrent and photovoltage decay experiments were performed on SQ2 samples in order to estimate $\eta_{coll}$ from exponential decay rates.[18] Without pyridine modification $\eta_{coll}$ was found to be 85.7%, whereas higher values of 92.2%, 92.1%, and 90.4% can be achieved with *t*BP, 4-MP, and mixed pyridines, respectively.

Further insights into the properties of the modified interfaces are provided by light intensity dependent current density-voltage measurements. Figure 3 shows the $J_{SC}$ of SQ2 solar cells with different pyridine configurations as a function of illumination intensity. Data are subjected to a power law fit $J_{SC} = \beta \cdot {P_0}^{\alpha}$, where $P_0$ is the illumination intensity and $\alpha$ and $\beta$ are fit parameters. As described in literature, the exponent $\alpha$ typically ranges between 0.75 and 1, where smaller values indicate limitations due to charge carrier recombination and built-up of space charge.[30]

For 4-MP modified interfaces we find slightly higher values of $\alpha$ indicating reduced recombination and more rapid charge transport away from the interface. Note that while differences in $\alpha$ among the tested devices are small, $100^{\alpha}$ increases by 5.2% and 3.3% for modification with 4-MP and mixed pyridines, respectively, compared to the device without pyridine. This implies that for light intensities in the order of one sun (100 mW $cm^{-2}$) these small differences in $\alpha$ reflect noticeable differences in short circuit current generation, although the overall impact of space charge seems to be small for all pyridine configurations.

In conclusion we show that significant performance increases can be achieved in hybrid solar cells with different sensitizer dyes and P3HT as hole transporter using the interfacial modifier 4-MP. We attribute this to favorable orientation of the P3HT at the $TiO_2$-polymer interface. When combining 4-MP with *t*BP, it is possible to simultaneously enhance $J_{SC}$ and $V_{OC}$ of the devices. Especially for dyes which allow a photocurrent contribution from the hole transporter the synergistic effect of the two pyridines plays an important role in pushing the efficiency. Contribution of the polymer to the charge generation is a prerequisite for taking advantage of the hybrid solar cell concept, making the combination of 4-MP and *t*BP interesting for this type of photovoltaic devices. Our detailed study on devices with a squaraine dye as a model system for such solar cells indicates that 4-MP improves the electronic properties of the inorganic-organic interface by promoting charge

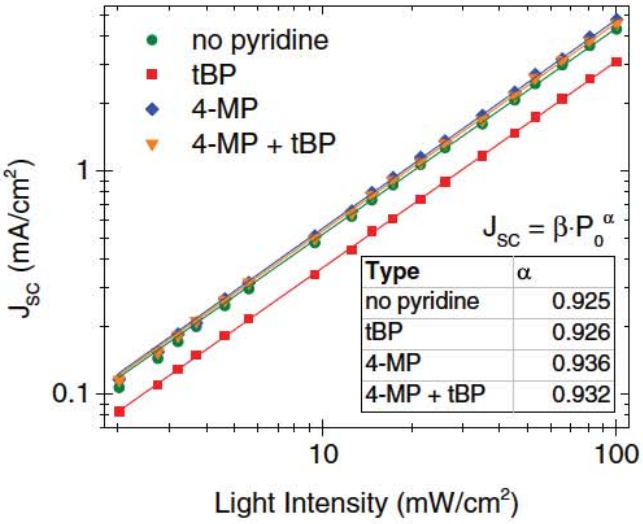


FIG. 3. $J_{SC}$ as a function of incident light intensity for SQ2 solar cells with different pyridine configurations. Lines represent results from power law fits.

separation and reducing charge recombination. From our findings we predict that design of suitable interfacial modifiers, which induce alignment of the hole transporter, is a pathway towards increased efficiencies of hybrid solar cells also for other p-type polymers as hole transporters.

We acknowledge support by the German Research Foundation (DFG) in the project "Identification and overcoming of loss mechanisms in nanostructured hybrid solar cells—pathways toward more efficient devices" and in the "SPP1355: Elementary processes of organic photovoltaics," the REFINE research consortium funded by the Carl Zeiss Foundation, and the Alexander von Humboldt Foundation. We thank Matthias Hagner for his help in the Nanostructure Laboratory at the University of Konstanz.

[1] S. D. Oosterhout, M. M. Wienk, S. S. van Bavel, R. Thiedmann, L. J. A. Koster, J. Gilot, J. Loos, V. Schmidt, and R. A. J. Janssen, Nature Mater. **8**(10), 818 (2009); B. A. Gregg, J. Phys. Chem. B **107**(20), 4688 (2003); J. Weickert, R. B. Dunbar, H. C. Hesse, W. Wiedemann, and L. Schmidt-Mende, Adv. Mater. **23**(16), 1810 (2011).
[2] W. Zhang, R. Zhu, F. Li, Q. Wang, and B. Liu, J. Phys. Chem. C **115**(14), 7038 (2011).
[3] R. Zhu, C. Y. Jiang, B. Liu, and S. Ramakrishna, Adv. Mater. **21**(9), 994 (2009).
[4] A. Abrusci, I. K. Ding, M. Al-Hashimi, T. Segal-Peretz, M. D. McGehee, M. Heeney, G. L. Frey, and H. J. Snaith, Energy Environ. Sci. **4**(8), 3051 (2011).
[5] W. J. E. Beek, M. M. Wienk, and R. A. J. Janssen, Adv. Mater. **16**(12), 1009 (2004); P. A. van Hal, M. M. Wienk, J. M. Kroon, W. J. H. Verhees, L. H. Slooff, W. J. H. van Gennip, P. Jonkheijm, and R. A. J. Janssen, *ibid.* **15**(2), 118 (2003); T.-W. Zeng, Y.-Y. Lin, H.-H. Lo, C.-W. Chen, C.-H. Chen, S.-C. Liou, H.-Y. Huang, and W.-F. Su, Nanotechnology **17**(21), 5387 (2006); M. Lira-Cantu and F. C. Krebs, Sol. Energy Mater. Sol. Cells **90**(14), 2076 (2006).
[6] S.-J. Moon, E. Baranoff, S. M. Zakeeruddin, C.-Y. Yeh, E. W.-G. Diau, M. Grätzel, and K. Sivula, Chem. Commun. **47**(29), 8244 (2011); A. Abrusci, R. S. S. Kumar, M. Al Hashimi, M. Heeney, A. Petrozza, and H. J. Snaith, Adv. Funct. Mater. **21**(13), 2571 (2011); Y. C. Huang, J. H. Hsu, Y. C. Liao, W. C. Yen, S. S. Li, S. T. Lin, C. W. Chen, and W. F. Su, J. Mater. Chem. **21**, 4450–4456 (2011).
[7] G. Dennler, M. C. Scharber, and C. J. Brabec, Adv. Mater. **21**(13), 1323 (2009); G. Li, R. Zhu, and Y. Yang, Nat. Photonics **6**(3), 153 (2012); G. Zhao, Y. He, and Y. Li, Adv. Mater. **22**(39), 4355 (2010).
[8] C. J. Brabec, N. S. Sariciftci, and J. C. Hummelen, Adv. Funct. Mater. **11**(1), 15 (2001).
[9] S. Hugger, R. Thomann, T. Heinzel, and T. Thurn-Albrecht, Colloid Polym. Sci. **282**(8), 932 (2004).
[10] G. Li, Y. Yao, H. Yang, V. Shrotriya, G. Yang, and Y. Yang, Adv. Funct. Mater. **17**(10), 1636 (2007).
[11] M. Aryal, K. Trivedi, and W. C. Hu, ACS Nano **3**(10), 3085 (2009).
[12] E. V. Canesi, M. Binda, A. Abate, S. Guarnera, L. Moretti, V. D'Innocenzo, R. S. S. Kumar, C. Bertarelli, A. Abrusci, H. Snaith, A. Calloni, A. Brambilla, F. Ciccacci, S. Aghion, F. Moia, R. Ferragut, C. Melis, G. Malloci, A. Mattoni, G. Lanzani, and A. Petrozza, Energy Environ. Sci. **5**(10), 9068 (2012).
[13] G. Boschloo, L. Häggman, and A. Hagfeldt, J. Phys. Chem. B **110**(26), 13144 (2006); R. Katoh, M. Kasuya, S. Kodate, A. Furube, N. Fuke, and N. Koide, J. Phys. Chem. C **113**(48), 20738 (2009).
[14] C. Goh, S. R. Scully, and M. D. McGehee, J. Appl. Phys. **101**(11), 114503 (2007).
[15] A. J. P. Carvalho and J. P. P. Ramalho, Appl. Surf. Sci. **256**(17), 5365 (2010).
[16] G. K. Mor, S. Kim, M. Paulose, O. K. Varghese, K. Shankar, J. Basham, and C. A. Grimes, Nano Lett. **9**(12), 4250 (2009).

[17] C. Tao, S. Ruan, G. Xie, X. Kong, L. Shen, F. Meng, C. Liu, X. Zhang, W. Dong, and W. Chen, Appl. Phys. Lett. **94**, 043311 (2009).
[18] See supplementary material at http://dx.doi.org/10.1063/1.4824040 for detailed experimental methods, JV characteristics, photoluminescence measurements, impedance spectroscopy fitting results, and PVD/PCD rates.
[19] Y. Vaynzof, D. Kabra, L. H. Zhao, P. K. H. Ho, A. T. S. Wee, and R. H. Friend, Appl. Phys. Lett. **97**(3), 033309 (2010).
[20] J. Weickert, F. Auras, T. Bein, and L. Schmidt-Mende, J. Phys. Chem. C **115**(30), 15081 (2011).
[21] Poly[2,1,3-benzothiadiazole-4,7-diyl[4,4-bis(2-ethylhexyl)-4H-cyclopenta[2,1-b:3,4-b′]dithiophene-2,6-diyl]].
[22] G. Grancini, R. S. S. Kumar, A. Abrusci, H.-L. Yip, C.-Z. Li, A.-K. Y. Jen, G. Lanzani, and H. J. Snaith, Adv. Funct. Mater. **22**(10), 2160 (2012).
[23] H. J. Snaith, Energy Environ. Sci. **5**(4), 6513 (2012).
[24] G. Malloci, M. Binda, A. Petrozza, and A. Mattoni, J. Phys. Chem. C **117**(27), 13894 (2013).
[25] N. S. Sariciftci, L. Smilowitz, A. J. Heeger, and F. Wudl, Science **258**(5087), 1474 (1992); M. Hallermann, S. Haneder, and E. Da Como, Appl. Phys. Lett. **93**(5), 053307 (2008); S. Sun, Z. Fan, Y. Wang, and J. Haliburton, J. Mater. Sci. **40**(6), 1429 (2005); W. U. Huynh, J. J. Dittmer, and A. P. Alivisatos, Science **295**(5564), 2425 (2002).
[26] F. Fabregat-Santiago, G. Garcia-Belmonte, I. Mora-Sero, and J. Bisquert, Phys. Chem. Chem. Phys. **13**(20), 9083 (2011).
[27] F. Fabregat-Santiago, J. Bisquert, L. Cevey, P. Chen, M. Wang, S. M. Zakeeruddin, and M. Grätzel, J. Am. Chem. Soc. **131**(2), 558 (2009).
[28] R. A. Street and M. Schoendorf, Phys. Rev. B **81** (20), 205307 (2010); P. P. Boix, G. Larramona, A. Jacob, B. Delatouche, I. Mora-Sero, and J. Bisquert, J. Phys. Chem. C **116**(1), 1579 (2012); M. M. Mandoc, F. B. Kooistra, J. C. Hummelen, B. De Boer, and P. W. M. Blom, Appl. Phys. Lett. **91**, 263505 (2007); J. P. Gonzalez-Vazquez, G. Oskam, and J. A. Anta, J. Phys. Chem. C **116**(43), 22687 (2012).
[29] L. Luo, C. J. Lin, C. S. Hung, C. F. Lo, C. Y. Lin, and E. W. G. Diau, Phys. Chem. Chem. Phys. **12**(40), 12973 (2010).
[30] L. J. A. Koster, V. D. Mihailetchi, H. Xie, and P. W. M. Blom, Appl. Phys. Lett. **87**, 203502 (2005); P. Schilinsky, C. Waldauf, and C. J. Brabec, *ibid.* **81**(20), 3885 (2002); V. D. Mihailetchi, H. X. Xie, B. de Boer, L. J. A. Koster, and P. W. M. Blom, Adv. Funct. Mater. **16**(5), 699 (2006).